

## Metallic phase in the metal-intercalated higher fullerene $\text{Rb}_{8.8(7)}\text{C}_{84}$

Yoshie Rikiishi,<sup>1,2</sup> Yoko Kashino,<sup>1</sup> Haruka Kusai,<sup>1</sup> Yasuhiro Takabayashi,<sup>1,2</sup> Eiji Kuwahara,<sup>1,2</sup> Yoshihiro Kubozono,<sup>1,2,3,\*</sup> Takashi Kambe,<sup>4</sup> Taishi Takenobu,<sup>2,5</sup> Yoshihiro Iwasa,<sup>2,5</sup> Naomi Mizorogi,<sup>6</sup> Shigeru Nagase,<sup>6</sup> and Susumu Okada<sup>7</sup>

<sup>1</sup>Department of Chemistry, Okayama University, Okayama 700-8530, Japan

<sup>2</sup>CREST, Japan Science and Technology Agency, Kawaguchi, 332-0012, Japan

<sup>3</sup>TARA Center, University of Tsukuba, Tsukuba 305-8577, Japan

<sup>4</sup>Department of Physics, Okayama University, Okayama 700-8530, Japan

<sup>5</sup>Institute for Materials Research, Tohoku University, Sendai 980-8577, Japan

<sup>6</sup>Institute for Molecular Science, Okazaki 444-8585, Japan

<sup>7</sup>Institute of Physics and Center for Computational Science, University of Tsukuba, Tsukuba 305-8577, Japan

(Received 31 December 2004; revised manuscript received 6 April 2005; published 30 June 2005)

A new material of higher fullerene,  $\text{Rb}_x\text{C}_{84}$ , was synthesized by intercalating Rb metal into  $\text{C}_{84}$  crystals. The  $\text{Rb}_x\text{C}_{84}$  crystals showed a simple cubic (sc) structure with lattice constant,  $a$ , of 16.82(2) Å at 6.5 K, and 16.87(2) Å at 295 K. The Rietveld refinements were achieved with the space group,  $Pa\bar{3}$ , based on a model that the  $C_2$  axis of  $D_{2d}\text{-C}_{84}$  aligned along [111]. The sample composition was determined to be  $\text{Rb}_{8.8(7)}\text{C}_{84}$ . The ESR spectrum at 303 K was composed of a broad peak with peak-to-peak linewidth  $\Delta H_{pp}$  of 220 G, and a narrow peak with  $\Delta H_{pp}$  of 24 G. Temperature dependence of the broad peak clearly showed a metallic behavior. The metallic behavior was discussed based on a theoretical calculation. This finding of new metallic phase in a higher fullerene is the first step for a development of new types of fullerene materials with novel physical properties such as superconductivity.

DOI: 10.1103/PhysRevB.71.224118

PACS number(s): 61.48.+c, 71.20.Tx, 72.80.Rj

### I. INTRODUCTION

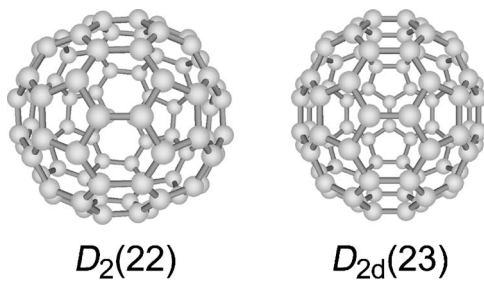
Alkaline metal intercalated  $\text{C}_{60}$  showed novel physical properties such as metallic behavior and superconductivity.<sup>1</sup> The highest superconducting transition temperature,  $T_c$ , was 33 K for  $\text{RbCs}_2\text{C}_{60}$ .<sup>2</sup> In spite of many efforts to find fullerene materials with higher  $T_c$ s, no higher  $T_c$  materials have yet been found except for  $\text{Cs}_3\text{C}_{60}$  with  $T_c$  of 40 K under 15 kbar.<sup>1,3</sup> The studies on new fullerene materials have so far been limited to  $\text{C}_{60}$  and  $\text{C}_{70}$  because of difficulty in obtaining pure solid samples.<sup>1</sup> Recently, crystalline solid samples of metallofullerenes and higher fullerenes were obtained, and their structures have been studied by x-ray powder diffractions.<sup>4–8</sup> The crystals of  $M@\text{C}_{82}$  ( $M$ =lanthanide atoms) showed a cubic structure of space group  $Pa\bar{3}$  [ $a$  = 15.78(1) Å for  $\text{Dy}@\text{C}_{82}$ , 15.78(1) Å for the  $C_{2v}$  isomer of  $\text{Ce}@\text{C}_{82}$ , and 15.74(4) Å for the  $C_s$  isomer of  $\text{Ce}@\text{C}_{82}$ ].<sup>5–7</sup> The photoemission (UPS),<sup>9</sup> resistivity  $\rho$ ,<sup>5,7,8</sup> optical spectroscopy<sup>10</sup> and scanning tunneling spectroscopy (STS) (Ref. 11) showed a semiconductorlike behavior with small energy gap,  $E_g$ , for  $M@\text{C}_{82}$  where the valence of  $M$  is +3. This result is not consistent with the theoretical prediction that  $M@\text{C}_{82}$  is metallic.<sup>12</sup>

The crystal structures of higher fullerenes,  $\text{C}_{76}$ ,  $\text{C}_{82}$ , and  $\text{C}_{84}$ , have been studied by x-ray diffraction with synchrotron radiation.<sup>13–15</sup> The crystals of the toluene-solvate of  $\text{C}_{76}$  and  $\text{C}_{82}$  showed a monoclinic lattice ( $a$  = 17.68 Å,  $b$  = 11.08 Å,  $c$  = 11.02 Å, and  $\beta$  = 108.10° for  $\text{C}_{76}$ , and  $a$  = 18.36 Å,  $b$  = 11.36 Å,  $c$  = 11.41 Å, and  $\beta$  = 108.07° for  $\text{C}_{82}$ ).<sup>13</sup> The solvent-free crystals of  $\text{C}_{82}$  showed a simple cubic structure (sc) [space group  $Pa\bar{3}$ ,  $a$  = 15.76(3) Å].<sup>14</sup> The crystals of the isomer-mixture of  $\text{C}_{84}$  showed a face-centered cubic structure (fcc) at 5–295 K.<sup>15</sup> The molecular symmetries of the

$\text{C}_{84}$  isomers were reported to be  $D_2$  and  $D_{2d}$ .<sup>16</sup> Allen *et al.* first succeeded in preparing crystalline samples of metal-doped higher fullerenes by K metal intercalation into the  $D_2$ - and  $D_{2d}\text{-C}_{84}$  crystals.<sup>17</sup> These crystals showed fcc structures with  $a$  of 16.536(6) Å for  $\text{K}_{8+x}\text{C}_{84}(D_{2d})$  and 16.561(7) Å for  $\text{K}_{8+x}\text{C}_{84}(D_2)$ .<sup>17</sup> Denning *et al.* reported fcc structures with  $a$  of 16.27(2) Å for  $\text{K}_{3.5(1)}\text{C}_{84}(D_{2d})$  and 16.34(1) Å for  $\text{K}_{2.6(1)}\text{C}_{84}(D_2)$ , and suggested the metallic behavior for these crystals.<sup>18</sup> Thus the metal-intercalated higher fullerenes have the highest potentiality towards a realization of novel physical properties among fullerenes. In the present study, we have fabricated a new metal-doped higher fullerene,  $\text{Rb}_x\text{C}_{84}$ . The crystal structure and electronic properties have been clarified by x-ray powder diffraction with synchrotron radiation and temperature dependent ESR.

### II. EXPERIMENT

The  $\text{C}_{84}$  samples were prepared by an arc-discharge of graphite rods containing  $\text{Eu}_2\text{O}_3$ . After Soxhlet-extraction of fullerenes with 1,2,4-trichlorobenzene,  $\text{C}_{84}$  was separated by a high performance liquid chromatography (HPLC) with a Buckyprep column; toluene was used as an eluent. Purified  $\text{C}_{84}$  samples were obtained by using a recycle system of HPLC. The sample purity of  $\text{C}_{84}$  was estimated to be ~99% by a time-of-flight (TOF) mass spectrometry. The  $\text{C}_{84}$  samples contained two isomers with molecular symmetries of  $D_2(22)$  and  $D_{2d}(23)$  where the notations in parenthesis refer to those used in Ref. 19. The molecular structures are shown in Fig. 1. These isomers are the most stable [ $D_{2d}(23)$ ] and the second most stable [ $D_2(22)$ ] among 24 isomers of  $\text{C}_{84}$  according to theoretical predictions.<sup>19,20</sup> The abundance

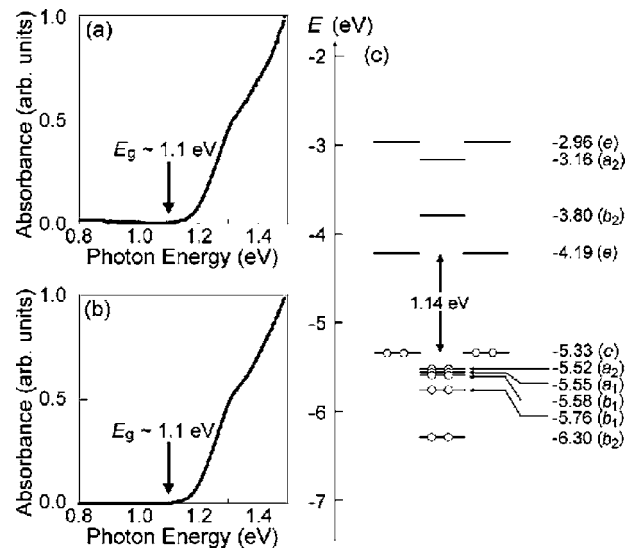
FIG. 1. Molecular structures of  $D_2(22)$ - and  $D_{2d}(23)$ - $C_{84}$ .

ratio of  $D_2(22)$  and  $D_{2d}(23)$  isomers was estimated to be 1:4 from the HPLC profile. Solvent-free samples of  $C_{84}$  were obtained by dynamic pumping under a pressure of  $10^{-5}$  Torr at 100 °C for 6 h, at 200 °C for 12 h and at 350 °C for 48 h. This process is similar to that for the preparation of solvent-free solids of  $C_{82}$ .<sup>14</sup>

Rb metal and the solvent-free sample of  $C_{84}$  were introduced into a glass tube in a glove box. The glass tube was sealed under a dynamic pumping at  $10^{-6}$  Torr. The  $Rb_xC_{84}$  sample was prepared by annealing at 623 K for 618 h. The x-ray diffraction pattern for the powder sample was measured with a synchrotron radiation of  $\lambda=1.0006$  Å at BL-1B of KEK-PF Tsukuba, Japan. The Rietveld refinement was carried out with the Rietan 2000 program developed by Izumi.<sup>21</sup> Temperature dependent ESR spectra were measured with an X-band ESR spectrometer (Bruker ESP300) equipped with an Oxford He flow cryostat.

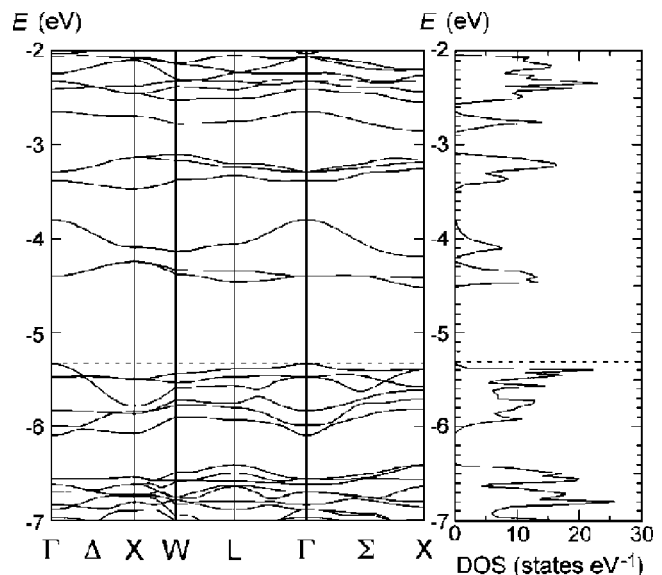
The calculation of the molecular orbital for pristine  $D_{2d}$ - $C_{84}$  was performed using density functional theory at the BLYP/3-21G level. The electronic energy band was determined by using the local density approximation (LDA) with the norm-conserving pseudopotential and the plane-wave basis set with the cutoff energy of 50 Ry. The energy band was calculated based on the fcc structure of  $C_{84}$  which is the same as the simple cubic structure of  $C_{84}$  ( $Pa\bar{3}$ ,  $Z=4$ ) except for the orientation of the  $C_{84}$  cage.

The energy gap of  $\sim 1.1$  eV opens in thin films of pristine  $C_{84}$ , as is seen from optical absorption spectra [Figs. 2(a) and 2(b)]. This value is consistent with that, 1.053 eV, estimated from the band calculation with density functional theory (DFT).<sup>22</sup> Further, the lowest unoccupied molecular orbital (LUMO) and the highest occupied molecular orbital (HOMO) calculated for the pristine  $D_{2d}$ - $C_{84}$  are twofold degenerate, respectively, and the HOMO-LUMO gap is 1.14 eV [Fig. 2(c)]. This value is also consistent with the optical gap of 1.1 eV. Therefore, the optical gap corresponds to the band gap of  $C_{84}$ . On the other hand, the gap energy of 0.55 eV was estimated from the plot of  $\ln \rho$  versus  $1/T$ .<sup>23</sup> Recently, Shiraishi *et al.* reported that the energy gap estimated from the  $\ln \rho - 1/T$  plot corresponds to the mobility gap of the thin films of  $C_{84}$ , where the mobility gap is defined as the energy difference between the actual Fermi level and the LUMO.<sup>24</sup> It should be noted that the actual Fermi level is located above the midpoint of the HOMO and the LUMO because  $C_{84}$  is an  $n$ -type semiconductor, as is suggested from the properties of the field-effect transistor (FET).<sup>23</sup> Actually, the energy gap of 0.55 eV observed from

FIG. 2. Optical absorption spectra of (a) mixture of  $D_2(22)$ - and  $D_{2d}(23)$ - $C_{84}$  and (b)  $D_{2d}(23)$ - $C_{84}$ . (c) Molecular orbital of  $D_{2d}(23)$ - $C_{84}$ .

the plot is  $\sim 1/2$  of the optical gap, i.e., the band gap. This result shows that pristine  $C_{84}$  is a normal semiconductor with small band gap of  $\sim 1.1$  eV.

Furthermore, the band calculation for the fcc  $D_{2d}$ - $C_{84}$  (Fig. 3) shows the existence of the narrow electronic band at  $-4.5$  to  $-4.2$  eV originating from a twofold degenerate  $e$  orbital, the broad band around  $-4$  eV due to the  $b_2$  orbital, and the narrow band at  $-3.5$  to  $-3.1$  eV originating from an  $a_2$  orbital and a twofold degenerate  $e$  orbital. Therefore, the alkaline metal doping into the  $C_{84}$  crystals should produce

FIG. 3. Electronic energy band and density of states (DOS) for the fcc  $D_{2d}$ - $C_{84}$ . Electrons are accommodated up to the dashed horizontal line. The midpoint between the LUMO and HOMO levels corresponds to the Fermi level when the  $C_{84}$  is assumed to be an intrinsic semiconductor. Actually, the exact Fermi level may be located above the midpoint because the  $C_{84}$  is an  $n$ -type semiconductor.

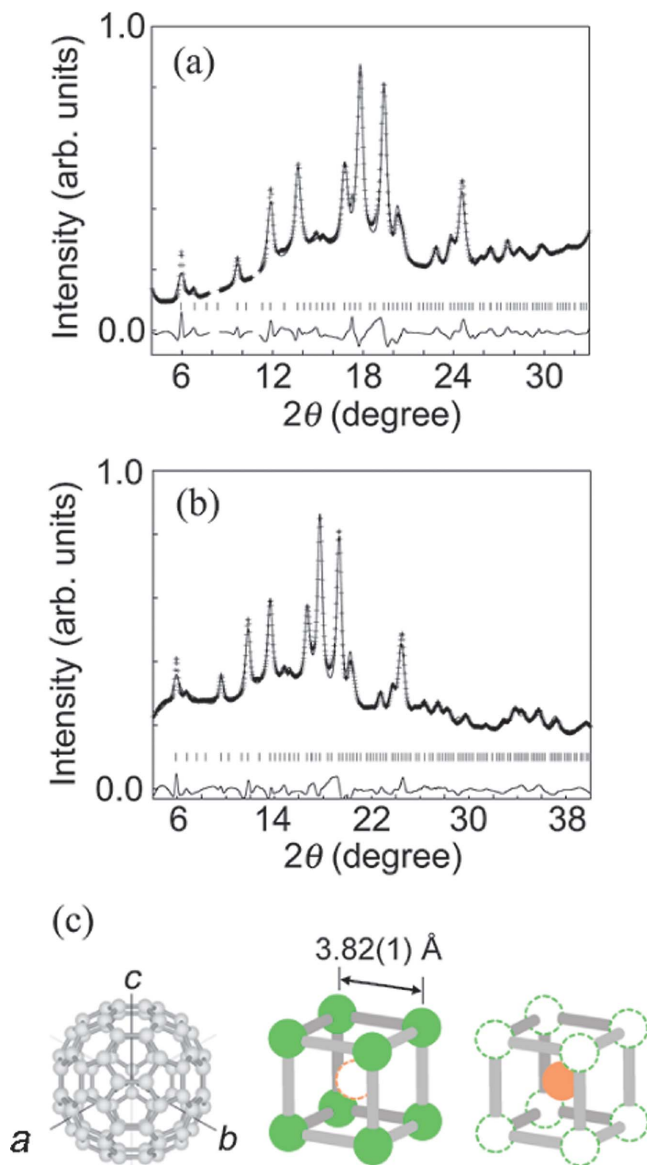


FIG. 4. (Color) X-ray diffraction patterns calculated with the structural parameters determined by Rietveld refinement (solid line) and the observed patterns (+ symbols) at (a) 6.5 and (b) 295 K. Allowed peak positions and the difference between the observed and calculated patterns are drawn by tick (middle) and solid line (bottom), respectively. (c) From left to right,  $D_{2d}(23)$ - $C_{84}$  molecule viewed along  $[111]$ , schematic representations of cube corners occupied by Rb and cube center occupied by Rb.

the electron-fillings for the above electronic bands.

### III. RESULTS AND DISCUSSION

The x-ray diffraction patterns of  $Rb_xC_{84}$  at 6.5 and 295 K are shown in Figs. 4(a) and 4(b). All Bragg reflections can be indexed as a cubic lattice with  $a$  of 16.82(2) Å at 6.5 K, and  $a$  of 16.87(2) Å at 295 K. These  $a$  values are larger by  $\sim 1$  Å than that for the  $D_{2d}$  and  $D_2$  isomer-mixture of  $C_{84}$ , 15.817(4) Å, at 20 K.<sup>15</sup> Furthermore, the  $a$  of 16.87(2) Å at 295 K is larger than the values determined for  $K_xC_{84}$

(16.27–16.34 Å for  $K_{-3}C_{84}$ , and 16.559 Å for  $K_{-8}C_{84}$ ). The  $a$  values for  $Rb_xC_{84}$  are the largest ones observed so far for the metal doped fullerenes and endohedral metallofullerenes.

In the x-ray diffraction pattern at 6.5 K, three reflections 4 3 0, 10 3 1, and 10 6 1 were observed, which do not satisfy the reflection condition for fcc ( $h+k, h+l, k+l=2n$ ). The occurrence of 4 3 0 reflection satisfies the reflection condition,  $h=2n$  for  $hk0$  for the general position,  $24d$ , of  $Pa\bar{3}$ . The other space group  $Pn\bar{3}$ , which was a candidate of the space group in some  $M@C_{82}$  crystals, requires the reflection condition,  $h+k=2n$  for  $hk0$ .<sup>5</sup> However, the occurrence of 4 3 0 reflection does not satisfy this condition. Furthermore, a trial of the Rietveld refinement with  $Pm\bar{3}$ , which has no reflection conditions, was not successful. Consequently, we carried out the Rietveld refinement with the space group  $Pa\bar{3}$  in the same manner as  $M@C_{82}$  and  $C_{82}$ .<sup>4–8,14</sup> The major phase,  $Rb_xC_{84}(D_{2d}(23))$ , was used in the refinement. The principal  $C_2$  axis of  $D_{2d}$ - $C_{84}$  extends along  $[111]$  [Fig. 4(c)]. The  $D_{2d}$ - $C_{84}$  molecule must be orientationally disordered around  $[111]$  to realize a cubic crystal, because the molecule has no 3 or  $\bar{3}$  symmetry.

In the unit cell, the 84 C atoms occupy  $24d$  position of the space group  $Pa\bar{3}$  with the occupancy factor of 1/6. The Rb can occupy four sites,  $(1/4, 1/4, 1/4)$ ,  $(1/2, 1/2, 1/2)$ ,  $(x, x, x)$ , and  $(x, x, 1-x)$ . The  $(1/4, 1/4, 1/4)$  and  $(1/2, 1/2, 1/2)$  sites are called the tetrahedral and octahedral sites, respectively, and correspond to the  $8c$  and  $4b$  positions, respectively. The  $(x, x, x)$  corresponds to  $8c$  position and  $(x, x, 1-x)$  to  $24d$  position. The C—C bond lengths in the  $D_{2d}(23)$ - $C_{84}$  were fixed at 1.36–1.47 Å. The temperature factors,  $B_s$ , of C and Rb, the occupancy factors of Rb, and  $x$  of Rb at the  $8c$  and  $24d$  positions were refined in the Rietveld refinement.

The calculated pattern for  $Rb_xC_{84}$  at 6.5 K is shown in Fig. 4(a) together with the experimental pattern. The calculated pattern reproduces well the experimental one. The final weighted pattern  $R$  factor,  $R_{wp}$ , and integrated intensity  $R$  factor,  $R_I$ , were 4.82% and 1.31%, respectively. The refined site occupancies for the Rb atoms were 74(3)% for the tetrahedral site, 17(5)% for the octahedral site, 89(2)% for the  $(x, x, x)$  and  $(x, x, 1-x)$  sites. The value of  $x$  was 0.3866(3), where the  $(x, x, x)$  and  $(x, x, 1-x)$  sites constitute the cube corners of the cubes around the respective octahedral sites, as shown in Fig. 4(c). The closest Rb—Rb distance in the cube is 3.82(1) Å. This value is larger than the closest K—K distance (face-diagonal) of 3.48(2) Å in  $K_{3.5(1)}C_{84}$  (Ref. 18) and that (cube-edge) of 3.631(2) Å in  $K_{8.39(17)}C_{84}$ .<sup>17</sup> This result reflects larger ionic radius of Rb than K. The closest Rb—Rb refers to cube edge sites as in  $K_{8.39(17)}C_{84}$  but does not refer to face-diagonal sites;<sup>17,18</sup> the corners of the cube are almost completely occupied by Rb atoms in the present phase. When the center of the cube is occupied by Rb, the closest Rb—Rb (center-corner) distance should be 3.31 Å. It is too small in comparison with the distance expected from the ionic radius of Rb. Therefore, the corner sites [green balls in Fig. 4(c)] can be expected to be vacant when the cube center is occupied by Rb [orange ball in Fig. 4(c)], and con-

TABLE I. Structural parameters of Rb in  $\text{Rb}_{8.8(7)}\text{C}_{84}$ .

$x$	$y$	$z$	$B$ ( $\text{\AA}^2$ )	Fractional occupancy (%)
		6.5 K		
1/4	1/4	1/4	11(2)	74(3)
1/2	1/2	1/2	27(15)	17(5)
0.3866(3)	0.3866(3)	0.3866(3)	2(2)	89(2)
0.3866(3)	0.3866(3)	0.6134(3)	13(2)	89(2)
		295 K		
1/4	1/4	1/4	9(1)	70(2)
1/2	1/2	1/2	22(15)	13(4)
0.3867(3)	0.3867(3)	0.3867(3)	9(5)	87(2)
0.3867(3)	0.3867(3)	0.6133(3)	11(2)	87(2)

versely the cube center should be vacant when the corner sites are occupied. If this is the case, the site occupancies of cube-corner and cube-center should be 8/9 ( $\sim 89\%$ ) and 1/9 ( $\sim 11\%$ ), respectively, whose values are consistent with the site occupancies, 89(2)% for the cube corner  $[(x,x,x)$  and  $(x,x,1-x)]$  and 17(5)% for the cube center  $[(1/2,1/2,1/2)]$ , determined by this Rietveld refinement.

From the Rietveld refinement, the  $x$  is determined to be 8.8(7) for  $\text{Rb}_x\text{C}_{84}$ . Similar phase was found in K-intercalated  $\text{C}_{84}$ , i.e.,  $\text{K}_{8.39(17)}\text{C}_{84}$  and  $\text{K}_{8.86(1)}\text{C}_{84}$ . The phase of  $\text{A}_{8.8(7)}\text{C}_{84}$  may be formed selectively because of the occupancies of 8/9 at  $(x,x,x)$  and  $(x,x,1-x)$  and that of 1/9 at  $(1/2,1/2,1/2)$  which are reasonable occupancies to prevent the Rb metal occupying both cube-center and cube-corners. These facts suggest that such stoichiometry corresponds to one of the stable phases in alkaline-metal doped  $\text{C}_{84}$  crystals.

The  $B$ s were  $1(2)\text{\AA}^2$  for C,  $11(2)\text{\AA}^2$  for Rb at  $(1/4,1/4,1/4)$ ,  $27(15)\text{\AA}^2$  for Rb at  $(1/2,1/2,1/2)$ ,  $2(2)\text{\AA}^2$  for Rb at  $(0.3866,0.3866,0.3866)$ , and  $13(2)\text{\AA}^2$  for Rb at  $(0.3866,0.3866,0.6134)$ . The  $B$  of C is close to that of  $\text{K}_3\text{C}_{60}$ ,  $1.2(5)\text{\AA}^2$ .<sup>25</sup> The large  $B$  of Rb at the  $(1/2,1/2,1/2)$  site originates from larger spatial site than the  $(1/4,1/4,1/4)$  site, as in the case of  $\text{K}_3\text{C}_{60}$ .<sup>25</sup> The Rietveld refinement by assuming coexistence of two phases of  $\text{Rb}_x\text{C}_{84}(D_{2d})$  and  $\text{Rb}_x\text{C}_{84}(D_2)$  was also tried, but further improvements were not obtained. In the Rietveld refinement with the space group  $P2_13$ , which is a maximal subgroup of  $P\bar{a}3$ , the  $B$  of C fell into negative value. Thus a possibility of the  $P2_13$  was rejected.

The Rietveld refinement was performed for the x-ray diffraction pattern at 295 K based on the structure at 6.5 K. The calculated pattern is shown in Fig. 4(b) together with the experimental one. The final  $R_{\text{wp}}$  and  $R_1$  were 3.66% and 1.73%, respectively. The site occupancies of Rb were 70(2)% at  $(1/4,1/4,1/4)$ , 13(4)% at  $(1/2,1/2,1/2)$ , 87(2)% at  $(x,x,x)$  and  $(x,x,1-x)$  sites. The composition can be estimated to be  $\text{Rb}_{8.4(5)}\text{C}_{84}$ . It is consistent with that,  $\text{Rb}_{8.8(7)}\text{C}_{84}$ , at 6.5 K within the standard uncertainty, and each site occupancy is also consistent with that at 6.5 K. This result shows that the occupancies determined by the Rietveld

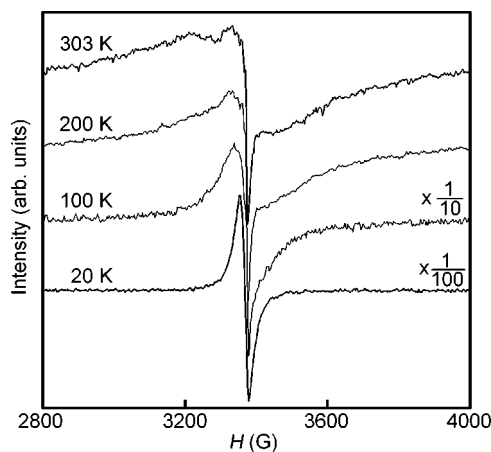
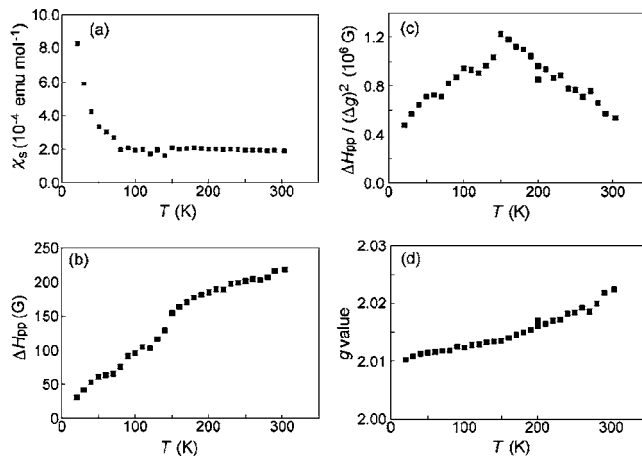


FIG. 5. Temperature-dependent ESR spectra at 20, 100, 200, and 303 K.

refinement are reliable. In the subsequent part of this paper we adopt  $\text{Rb}_{8.8(7)}\text{C}_{84}$  determined at 6.5 K as the composition of the sample. The  $B$  of C increased from  $1(2)\text{\AA}^2$  at 6.5 K to  $3(1)\text{\AA}^2$  at 295 K. The  $B$ s of Rb were almost constant even when the temperature was changed from 6.5 to 295 K, which shows that the  $B$ s of Rb are substantially defined by a static disorder. Structural parameters of Rb are listed in Table I.

Temperature-dependent ESR spectra for  $\text{Rb}_{8.8(7)}\text{C}_{84}$  are shown in Fig. 5. The ESR spectrum at 303 K is composed of at least two peaks, and the spectrum was analyzed with two Lorentz peaks. The peak-to-peak linewidth,  $\Delta H_{pp}$ , for the broad peak is 220 G. The  $\Delta H_{pp}$  is smaller than that for  $\text{Rb}_3\text{C}_{60}$ , 490 G,<sup>26</sup> while it is much larger than the values for  $\text{K}_x\text{C}_{84}$  [ $\sim 4$  G for  $\text{K}_{2.6(1)}\text{C}_{84}(D_2)$ ,  $\sim 6$  G for  $\text{K}_{3.5(1)}\text{C}_{84}(D_{2d})$ , and 3.5 G for  $\text{K}_{8.86(11)}\text{C}_{84}(D_{2d}+D_2)$ ].<sup>17,18</sup> The  $\Delta H_{pp}$  for the narrow peak is 24 G at 303 K. The broad spectrum becomes narrower with decreasing temperature (Fig. 5). The temperature dependence of spin susceptibility,  $\chi_s$ , estimated from the broad peak is shown in Fig. 6(a). The  $\chi_s$  shows a constant value down to 80 K, suggesting a Pauli-type  $\chi_s$ . The intensity of the narrow peak increased drastically at low tempera-

FIG. 6. Temperature dependence of (a)  $\chi_s$ , (b)  $\Delta H_{pp}$ , (c)  $\Delta H_{pp}/(\Delta g)^2$ , and (d)  $g$ .

ture, showing a Curie-type behavior and a small Curie constant of  $1.4 \times 10^{-3}$  emu K mol $^{-1}$ ; the  $\Delta H_{pp}$  of the narrow peak was constant at 20–303 K. Thus it was difficult to extract the exact intensity of the broad peak owing to an existence of the intense narrow peak at low temperature. Therefore the intensity of the broad peak increased apparently at low temperature, due to the narrow peak ascribed to the defect spin. Thus the intensity of the broad peak is expected to be constant even below 80 K.

The  $\Delta H_{pp}$  estimated from the broad peak linearly increases with an increase in temperature [Fig. 6(b)]. This result shows that the phase of  $\text{Rb}_{8.8(7)}\text{C}_{84}$  is metallic. The temperature dependence of  $\Delta H_{pp}$  for  $\text{Rb}_{8.8(7)}\text{C}_{84}$  is consistent with those for  $\text{K}_{3.5(1)}\text{C}_{84}$  and  $\text{K}_{2.7(1)}\text{C}_{84}$  which are concluded to be metallic.<sup>18</sup> Elliot showed that  $\Delta H_{pp}$  was related to the  $g$  shift,  $\Delta g$ , relative to the  $g$  value, 2.0023, of the free electron as  $\Delta H_{pp} \sim (\Delta g)^2 / \tau$  when the dominant contribution to spin-lattice relaxation rate was the modulation of spin-orbit interactions by phonon;  $\tau$  is relaxation time in the Drude model.<sup>27,28</sup> The  $\Delta H_{pp}$  of three-dimensional (3D) conventional metals follows the above expression. Here it should be noted that the  $\Delta H_{pp} / (\Delta g)^2$  is proportional to  $\rho$  in the 3D metals. The plot of  $\Delta H_{pp} / (\Delta g)^2$  versus  $T$  is shown in Fig. 6(c). The  $\Delta H_{pp} / (\Delta g)^2$  value increases linearly with increasing temperature up to 150 K, showing clearly metallic behavior. A drastic change is observed around 150 K in this plot. Above 150 K the  $\Delta H_{pp} / (\Delta g)^2$  value decreases monotonically up to 300 K. Such a change was not observed in plots of  $\chi_s$  and  $\Delta H_{pp}$  versus  $T$  [Figs. 6(a) and 6(b)]. On the other hand, a linear relationship was found in the  $\Delta H_{pp} / (\Delta g)^2$  plots in  $\text{Rb}_3\text{C}_{60}$ ,  $\text{K}_3\text{C}_{60}$ , and  $\text{Na}_2\text{CsC}_{60}$  which are recognized to be metallic.<sup>26</sup> The drastic change in the plot of  $\Delta H_{pp} / (\Delta g)^2$  versus  $T$  is caused by a rapid increase in  $g$  value above 150 K [Fig. 6(d)]. Such a rapid increase in  $g$  was observed in  $\text{Cs}_{3.3(1)}\text{C}_{60}$ .<sup>29</sup> The variation of temperature dependence of  $g$  and  $\Delta H_{pp} / (\Delta g)^2$  may imply the presence of a structural phase transition or change of molecular motion, because the  $g$  value is sensitive to structural variation around the conduction electron. However, no structural phase transitions were observed in  $\text{C}_{84}$  below 300 K.<sup>15</sup> This fact does not actively support the presence of the structural phase transition in  $\text{Rb}_{8.8(7)}\text{C}_{84}$ . Thus the temperature dependent-ESR suggests that  $\text{Rb}_{8.8(7)}\text{C}_{84}$  is metallic, but the origin of the variation of temperature dependence of  $g$  and  $\Delta H_{pp} / (\Delta g)^2$  remains to be clarified.

The MO calculation for the pristine  $D_{2d}(23)\text{-C}_{84}$  shown in Fig. 2(c) suggests that the twofold degenerate  $e$  orbital at  $-2.96$  eV is singly occupied in  $\text{Rb}_{8.8(7)}\text{C}_{84}$  because of  $\sim 9$  electron-transfer from Rb to  $\text{C}_{84}$ . The theoretical density of states (DOS) for fcc  $D_{2d}\text{-C}_{84}$  calculated for the band at  $-3.3$  to  $-3.1$  eV is close to that for the band at  $-4.5$  to  $-4.2$  eV, as seen from Fig. 3. The band at  $-3.3$  to  $-3.1$  eV corresponds to the twofold degenerate  $e$  orbital and the band is partial-filled in  $\text{Rb}_{8.8(7)}\text{C}_{84}$ . The narrow electronic band at  $-4.5$  to  $-4.2$  eV should be partial-filled in  $\text{K}_{3.5(1)}\text{C}_{84}$  and  $\text{K}_{2.7(1)}\text{C}_{84}$ . The theoretical calculation (Fig. 3) predicts that

the DOS on the Fermi level,  $D(\epsilon_F)$ , for  $\text{Rb}_{8.8(7)}\text{C}_{84}$  is close to those for  $\text{K}_{3.5(1)}\text{C}_{84}$  and  $\text{K}_{2.7(1)}\text{C}_{84}$ , if the doping causes no significant modification of the energy band.

The broad ESR peak (Fig. 5) could be assigned to the conduction electron ESR ( $c$ -ESR); the broad spectrum was analyzed with Lorentz line shape. It should be noted that the  $c$ -ESR spectrum does not show a Dysonian line shape because this sample is fine crystals. The  $\chi_s$  of  $\text{Rb}_{8.8(7)}\text{C}_{84}$  estimated from the broad peak at 303 K was  $1.9 \times 10^{-4}$  emu mol $^{-1}$  which corresponds to the Pauli susceptibility. The  $D(\epsilon_F)$  was estimated to be 2.9 states eV $^{-1}$   $\text{C}_{84}^{-1}$  spin $^{-1}$  from the  $\chi_s$ . This value is close to those for  $\text{K}_{3.5(1)}\text{C}_{84}$  (2.01 states eV $^{-1}$   $\text{C}_{84}^{-1}$  spin $^{-1}$ ) and  $\text{K}_{2.7(1)}\text{C}_{84}$  (2.63 states eV $^{-1}$   $\text{C}_{84}^{-1}$  spin $^{-1}$ ),<sup>18</sup> as is expected from the theoretical calculation (Fig. 3). The slight increase in  $D(\epsilon_F)$  of  $\text{Rb}_{8.8(7)}\text{C}_{84}$  in comparison to those for  $\text{K}_{3.5(1)}\text{C}_{84}$  and  $\text{K}_{2.7(1)}\text{C}_{84}$  is probably due to the lattice expansion from  $\sim 16.3$  Å to 16.87(2) Å.

The synthesis of the fullerene material,  $\text{Rb}_{8.8(7)}\text{C}_{84}$ , with the largest  $a$  among metal doped fullerenes and endohedral metallofullerenes was of significance for a realization of superconductors based on fullerenes other than  $\text{C}_{60}$ , because the large  $D(\epsilon_F)$  is expected owing to the small transfer integral between the fullerene molecules. However, the  $D(\epsilon_F)$  value of  $\text{Rb}_{8.8(7)}\text{C}_{84}$ , 2.9 states eV $^{-1}$   $\text{C}_{84}^{-1}$  spin $^{-1}$ , is smaller than those of  $\text{K}_3\text{C}_{60}$  (14 states eV $^{-1}$   $\text{C}_{60}^{-1}$  spin $^{-1}$ ),  $\text{Rb}_3\text{C}_{60}$  (19 states eV $^{-1}$   $\text{C}_{60}^{-1}$  spin $^{-1}$ ), and  $\text{Cs}_3\text{C}_{60}$  (9 states eV $^{-1}$   $\text{C}_{60}^{-1}$  spin $^{-1}$ ).<sup>30,31</sup> The small  $D(\epsilon_F)$  of  $\text{Rb}_{8.8(7)}\text{C}_{84}$  may not lead to a significant  $T_c$  in the BCS model, and the superconducting transition could not be observed down to 2 K. Furthermore, the structural disorder that two isomers of  $D_{2(22)}$  and  $D_{2d}(23)\text{-C}_{84}$  are contained in this sample may be responsible for no observation of superconductivity in  $\text{Rb}_{8.8(7)}\text{C}_{84}$ . In fact it is suggested that the existence of two phases, body-centered orthorhombic and cubic, destroys the superconductivity in  $\text{Cs}_3\text{C}_{60}$  under ambient pressure.<sup>3,29</sup> Thus, the structural disorder will not produce a positive effect for an appearance of superconductivity. Nevertheless, the finding of a new metallic phase in metal doped higher fullerene is very important for the development of new carbon-cluster materials with novel physical properties.

The  $\chi_s$  due to defect spin,  $3.6 \times 10^{-6}$  emu mol $^{-1}$ , estimated from the narrow peak of the ESR at 303 K is smaller by two orders of magnitudes than the  $\chi_s$  ascribable to Pauli susceptibility,  $1.9 \times 10^{-4}$  emu mol $^{-1}$ . The Curie constant for the  $\chi_s$  due to the defect spin results in a very small unpaired electron,  $4 \times 10^{-3}$  spin per  $\text{C}_{84}$ , whose value is smaller than those of  $\text{K}_x\text{C}_{84}$ , 0.1–0.3 per  $\text{C}_{84}$ .<sup>17,18</sup> This implies that the  $\text{Rb}_{8.8(7)}\text{C}_{84}$  sample has less defects than  $\text{K}_x\text{C}_{84}$ . Recently, it was found that  $M@\text{C}_{82}$  is not metallic but semiconductor-like, regardless of the fact that odd numbers of electrons are transferred to the  $\text{C}_{82}$  cage from the encapsulated metal atom.<sup>5–11</sup> However, the metallic behavior found in  $\text{Rb}_{8.8(7)}\text{C}_{84}$  can be explained by the simple band picture, as in the case of alkaline metal doped  $\text{C}_{60}$ .<sup>1</sup> This indicates the possibility of materials design with higher fullerenes conducted by theoretical calculation.

## ACKNOWLEDGMENTS

The authors acknowledge Professor Mototada Kobayashi of University of Hyogo for his valuable suggestion in x-ray diffraction measurements, and Miss Rie Watanabe of Okayama University for her kind assistance in sample preparation. The x-ray diffraction study was performed under the

proposal of KEK-PF, 2002G201. This work was supported by a Grant-in-Aid (15350089) from the Ministry of Education, Culture, Sports, Science and Technology of Japan, by Okayama University COE Project, by the Mitsubishi Foundation, and by the Visiting Researcher's program Institute for Materials Research of Tohoku University (2003).

\*Electronic mail: kubozone@cc.okayama-u.ac.jp

- <sup>1</sup>Y. Iwasa and Y. Takenobu, *J. Phys.: Condens. Matter* **15**, R495 (2003).
- <sup>2</sup>K. Tanigaki, T. W. Ebbesen, S. Saito, J. Mizuki, J. S. Tsai, Y. Kubo, and S. Kuroshima, *Nature (London)* **352**, 222 (1991).
- <sup>3</sup>T. T. M. Palstra, O. Zhou, Y. Iwasa, P. E. Sulewski, R. M. Fleming, and B. R. Zegarski, *Solid State Commun.* **93**, 327 (1995).
- <sup>4</sup>Y. Takabayashi, Y. Kubozono, T. Kanbara, S. Fujiki, K. Shibata, Y. Haruyama, T. Hosokawa, Y. Rikiishi, and S. Kashino, *Phys. Rev. B* **65**, 073405 (2002).
- <sup>5</sup>Y. Kubozono, Y. Takabayashi, K. Shibata, T. Kanbara, S. Fujiki, S. Kashino, A. Fujiwara, and S. Emura, *Phys. Rev. B* **67**, 115410 (2003).
- <sup>6</sup>K. Shibata, Y. Rikiishi, T. Hosokawa, Y. Haruyama, Y. Kubozono, S. Kashino, T. Uruga, A. Fujiwara, H. Kitagawa, T. Takano, and Y. Iwasa, *Phys. Rev. B* **68**, 094104 (2003).
- <sup>7</sup>Y. Rikiishi, Y. Kubozono, T. Hosokawa, K. Shibata, Y. Haruyama, Y. Takabayashi, A. Fujiwara, S. Kobayashi, S. Mori, and Y. Iwasa, *J. Phys. Chem. B* **108**, 7580 (2004).
- <sup>8</sup>T. Hosokawa, S. Fujiki, E. Kuwahara, Y. Kubozono, H. Kitagawa, A. Fujiwara, T. Takenobu, and Y. Iwasa, *Chem. Phys. Lett.* **395**, 78 (2004).
- <sup>9</sup>S. Hino, H. Takahashi, K. Iwasaki, K. Matusmoto, T. Miyazaki, S. Hasegawa, K. Kikuchi, and Y. Achiba, *Phys. Rev. Lett.* **71**, 4261 (1993).
- <sup>10</sup>C. J. Nuttall, Y. Hayashi, K. Yamazaki, T. Mitani, and Y. Iwasa, *Adv. Mater. (Weinheim, Ger.)* **14**, 293 (2002).
- <sup>11</sup>S. Fujiki, Y. Kubozono, Y. Rikiishi, and T. Urisu, *Phys. Rev. B* **70**, 235421 (2004).
- <sup>12</sup>S. Amamiya, S. Okada, S. Suzuki, and K. Nakao, *Synth. Met.* **121**, 1137 (2001).
- <sup>13</sup>H. Kawada, Y. Fujii, H. Nakao, Y. Murakami, T. Watanuki, H. Suematsu, K. Kikuchi, Y. Achiba, and I. Ikemoto, *Phys. Rev. B* **51**, 8723 (1995).
- <sup>14</sup>Y. Kubozono, Y. Rikiishi, K. Shibata, T. Hosokawa, S. Fujiki, and H. Kitagawa, *Phys. Rev. B* **69**, 165412 (2004).
- <sup>15</sup>S. Margadonna, C. M. Brown, T. J. S. Dennis, A. Lappas, P. Pattison, K. Prassides, and H. Shinohara, *Chem. Mater.* **10**, 1742 (1998).
- <sup>16</sup>T. J. S. Dennis, T. Kai, T. Tomiyama, and H. Shinohara, *Chem. Commun. (Cambridge)* **1998**, 619.
- <sup>17</sup>K. M. Allen, T. J. S. Dennis, M. J. Rosseinsky, and H. Shinohara, *J. Am. Chem. Soc.* **120**, 6681 (1998).
- <sup>18</sup>M. S. Denning, T. J. S. Dennis, M. J. Rosseinsky, and H. Shinohara, *Chem. Mater.* **13**, 4753 (2001).
- <sup>19</sup>P. W. Fowler and D. E. Manolopoulos, *An Atlas of Fullerenes* (Clarendon, Oxford, 1995).
- <sup>20</sup>K. Kobayashi, and S. Nagase, in *Endofullerenes: A New Family of Carbon Clusters*, edited by T. Akasaka and S. Nagase (Kluwer Academic, Dordrecht, 2002), p. 99.
- <sup>21</sup>F. Izumi, in *The Rietveld Method*, edited by R. A. Young (Oxford University Press, Oxford, 1993), p. 236.
- <sup>22</sup>S. Saito, S. Sawada, N. Hamada, and A. Oshiyama, *Jpn. J. Appl. Phys., Part 1* **32**, 1438 (1993).
- <sup>23</sup>K. Shibata, Y. Kubozono, T. Kanbara, T. Hosokawa, A. Fujiwara, Y. Ito, and H. Shinohara, *Appl. Phys. Lett.* **84**, 2572 (2004).
- <sup>24</sup>M. Shiraishi, K. Shibata, R. Maruyama, and M. Ata, *Phys. Rev. B* **68**, 235414 (2003).
- <sup>25</sup>P. W. Stephens, L. Mihaly, P. L. Lee, R. L. Whetten, S.-M. Huang, R. Kaner, F. Deiderich, and K. Holczer, *Nature (London)* **351**, 632 (1991).
- <sup>26</sup>P. Petit, J. Robert, T. Yildirim, and J. E. Fischer, *Phys. Rev. B* **54**, R3764 (1996).
- <sup>27</sup>R. J. Elliott, *Phys. Rev.* **96**, 266 (1954).
- <sup>28</sup>L. Alcacer, in *Organic Conductors, Fundamentals and Applications*, edited by J.-P. Farges (Marcel Dekker, New York, 1994), p. 269.
- <sup>29</sup>S. Fujiki, Y. Kubozono, M. Kobayashi, T. Kambe, Y. Rikiishi, S. Kashino, K. Ishii, H. Suematsu, and A. Fujiwara, *Phys. Rev. B* **65**, 235425 (2002).
- <sup>30</sup>A. P. Ramirez, *Supercond. Rev.* **1**, 1 (1994).
- <sup>31</sup>Y. Kubozono, S. Fujiki, K. Hiraoka, T. Urakawa, Y. Takabayashi, S. Kashino, Y. Iwasa, T. Kitagawa, and Y. Mitani, *Chem. Phys. Lett.* **298**, 335 (1998).